

Patterns of mammalian population decline inform conservation action

Journal:	<i>Journal of Applied Ecology</i>
Manuscript ID	JAPPL-2015-00160.R2
Manuscript Type:	Standard Paper
Date Submitted by the Author:	n/a
Complete List of Authors:	Di Fonzo, Martina; University of Queensland, Centre for Biodiversity and Conservation Science; Collen, Ben; Institute of Zoology, Chauvenet, Alienor; University of Queensland, Centre for Biodiversity and Conservation Science Mace, Georgina; University College London, Genetics, Evolution and Environment
Key-words:	extinction risk, indicators, mammals, population decline, time-series analysis, monitoring, management

1 **Patterns of mammalian population decline inform conservation action**

2 Martina M. I. Di Fonzo^{1,2,3*}, Ben Collen⁴, Alienor L. M. Chauvenet³ and Georgina M. Mace^{2,4}

3

4 1. Institute of Zoology, Zoological Society of London, Regent's Park, London, NW1 4RY,
5 United Kingdom

6 2. Division of Ecology and Evolution, Imperial College London, Silwood Park, Ascot, SL5
7 7PY, United Kingdom

8 3. ARC Centre of Excellence for Environmental Decisions, the NERP Environmental Decisions
9 Hub, Centre for Biodiversity and Conservation Science, University of Queensland, Brisbane,
10 Queensland 4072, Australia; email: m.difonzo@uq.edu *

11 4. Department of Genetics, Evolution and Environment, Centre for Biodiversity & Environment
12 Research, University College London, Gower Street, London, WC1E 6BT, United Kingdom

13

14 *current address

15

16 **Running title:** Patterns of decline inform conservation action

17 **Word count:** Summary (318), Main text (3696), Acknowledgements (99), References (1512), Tables
18 and Figure legends (434), Data accessibility information (241) **Total: 6301**

19 **Number of tables and figures in main text:** 5 tables and 2 figures

20 **Number of references:** 52

21

22

23 SUMMARY

- 24 1. Evaluations of wildlife population dynamics have the potential to convey valuable
25 information on the type of pressure affecting a population and could help predict future
26 changes in the population's trajectory. Greater understanding of different patterns of
27 population declines could provide a useful mechanism for assessing decline severity in the
28 wild and identifying those populations that are more likely to exhibit severe declines.
- 29 2. We identified 93 incidences of decline within 75 populations of mammalian species using a
30 time-series analysis method. These included: linear, quadratic convex (accelerating) declines,
31 exponential concave (decelerating) declines, and quadratic concave declines (representing
32 recovering populations). Excluding linear declines left a dataset of 85 declines to model the
33 relationship between each decline-curve type and a range of biological, anthropogenic, and
34 time-series descriptor explanatory variables.
- 35 3. None of the decline-curve types were spatially or phylogenetically clustered. The only
36 characteristic that could be consistently associated with any curve-type was the time at which
37 they were more likely to occur within a time-series. Quadratic convex declines were more
38 likely to occur at the start of the time-series, while recovering curve shapes (quadratic
39 concave declines) were more likely at the end of the time-series.
- 40 4. **Synthesis and applications:** The ability to link certain factors with specific decline
41 dynamics across a number of mammalian populations is useful for management purposes as it
42 provides decision-makers with potential triggers upon which to base their conservation
43 actions. We propose that the identification of quadratic convex declines could be used as an
44 early-warning signal of potentially severe decline dynamics. For such populations, increased
45 population monitoring effort should be deployed to diagnose the cause of its decline and avert
46 possible extinctions. Conversely, the presence of a quadratic concave decline suggests that
47 the population has already undergone a period of serious decline but is now in the process of
48 recovery. Such populations will require different types of conservation actions, focussed on
49 enhancing their chances of recovery.

50 **Key words:** Extinction risk; indicators; monitoring; mammals, population decline; time-series
51 analysis, management

52

53

54 INTRODUCTION

55 Wildlife monitoring programmes play a key role in understanding ecological systems, and
56 constitute the basis for management decisions and actions (Yoccoz, Nichols & Boulinier 2001). As
57 well as tracking a species' status in the wild, long-term population studies provide an insight into a
58 population's usual abundance and variability prior to anthropogenic activity, and can be used to
59 determine whether a decline is part of a natural cycle or the result of external pressure (Willis *et al.*
60 2007). Monitoring population declines is an especially important step in tackling biodiversity loss, as
61 severe population reductions act as a prelude to species extinction (Ceballos & Ehrlich 2002; Collen
62 *et al.* 2009). Yet, a recent study has raised concern over the number of monitoring programmes that
63 have “monitored populations to extinction”, with no clear guidelines on how to act when declines are
64 first diagnosed (Lindenmayer, Pigott & Wintle 2013). Here we explore how differences in decline
65 shape could represent useful “triggers points” within monitoring programmes, highlighting when and
66 where rapid management intervention is called.

67

68 Recent analyses across a set of a long-term mammalian population time-series have revealed
69 several key distinctions in wildlife population declines (Di Fonzo, Collen & Mace 2013), which
70 provide a more nuanced understanding of extinction risk compared with simple measures of average
71 population change or cumulative percentage loss (i.e. Criterion A of the Red List; IUCN 2001). Di
72 Fonzo *et al.* (2013) identified three principal decline-curve types of increasing severity: quadratic
73 concave (i.e. recovering), exponential concave (i.e. decelerating) and quadratic convex (i.e.
74 accelerating) decline-curves (Fig. 1 a-b.; Table S1), that carry information regarding the potential
75 urgency of conservation interventions. Moreover, there is some evidence that dominant threats can be

76 diagnosed from distinctions in long-term abundance trend data using flexible Bayesian frameworks
77 (Shoemaker & Akçakaya 2015).

78 In order to evaluate whether these decline-types represent useful triggers for conservation
79 action, we must first determine whether their presence is associated with any particular biological,
80 environmental or anthropogenic conditions. While it is well known that certain biological and
81 ecological attributes predispose species to higher extinction risk (e.g. large body size, low population
82 density, small geographic range, specific dietary requirements; Purvis *et al.* 2000), recent studies have
83 revealed limited associations between intrinsic traits and population level trends (Cowlshaw, Pettifor
84 & Issac 2009; Mace *et al.* 2010; Collen *et al.* 2011). Instead, they find site-specific characteristics
85 (such as anthropogenic pressure intensity or certain environmental conditions) to be better
86 determinants of population decline. Although these studies do not identify any link between negative
87 population trends and species with an intrinsically higher risk of extinction, this does not preclude
88 associations with specific decline-types. For instance, species at a greater risk of extinction could
89 exhibit a higher frequency of severe quadratic convex declines, which might have been missed in
90 previous population trend analyses (i.e. based on simple linear regression). A higher frequency of
91 switching between accelerating quadratic convex declines and recovering concave trajectories (i.e.
92 exhibited during the process of “critical slowing down” prior to catastrophic declines; Scheffer *et al.*
93 2009; Drake & Griffen 2010) is a further potential indicator of proximate extinction, which could be
94 built within monitoring programmes to rapidly tackle at-risk populations before it is too late.

95 In this study we investigate the association between the decline-curve dynamics of a sample
96 of mammalian population data from a database of vertebrate abundance time-series and a range of
97 characteristics (defined in Table 1). Specifically, we use generalised linear mixed modelling to
98 investigate whether the presence of different decline-curve types is dependent on particular species-
99 specific traits, levels of local, anthropogenic pressure, or based on particular attributes of the time-
100 series itself. Through this study, we hope to provide insight into the conditions contributing to
101 different decline-curves, which could be used to pre-empt the application of particular conservation
102 management strategies. We chose to focus our study on mammals as they are a very well-monitored

103 and extensively studied vertebrate group, with a quarter of species recorded to be threatened with
104 extinction (Schipper *et al.* 2008).

105

106

107 **MATERIALS AND METHODS**

108 ***Data manipulation***

109 We first selected 75 high quality mammalian population time-series for our analysis,
110 representing 33 species, spanning 6 orders, which we drew from a vertebrate population abundance
111 database (Living Planet Database (LPD); Collen *et al.* 2009) based on criteria from Di Fonzo *et al.*
112 (2013). The minimum requirement was that time-series had population counts which spanned more
113 than 5 years, had less than 8 year gap between data points, were collected from 1900 onwards,
114 exhibited stable or declining abundance trends (using linear regression), exhibited low environmental
115 stochasticity (based on whether the total reduction in population abundance was less than the
116 difference between the upper and lower 95% confidence interval around the linear model fit), and
117 were reported as being affected by one or more threats in the original source. All the data
118 manipulation and analyses here after were carried out using the statistical programming software, R
119 3.1.0 (R Development Core Team 2015).

120 We then applied the Kalman filter (as used by Knape & de Valpine 2012) to the time-series
121 data to account for potential sources of uncertainty arising from count errors using the ‘dlmMLE’
122 function (‘dlm’ package; Petris 2015) Next, we identified the different decline-curves using the
123 following steps, described in Di Fonzo *et al.* (2013), and summarised as follows : 1) we smoothed the
124 Kalman-filtered time-series using a generalised additive modelling framework (Wood 2006); 2)
125 detected statistically significant switches in dynamics (which we term ‘switch points’) based on
126 changes in the trend’s second derivative sign (fully described in Di Fonzo *et al.* 2013); and 3) fit a
127 range of algebraic functions between switch points to determine the different curve-types based on

128 lowest Akaike Information Criterion corrected for small sample size (AICc; Sugiura 1978), based on a
129 threshold of 4 AICc (Burnham & Anderson 2004). We excluded 8 linear declines from the dataset as
130 these decline types could not be robustly associated with a specific pressure-type (Di Fonzo, Collen &
131 Mace 2013). This left us with 85 decline-curve types (35 quadratic convex, 29 quadratic concave and
132 21 exponential concave) from 60 high quality mammalian population time-series, distributed around
133 the globe (Fig.2; Table S2 in Supporting Information). The above analyses were carried out using the
134 following R packages: 'AICcmodavg,' (Mazerolle 2015), 'mgcv' (Wood 2006), 'timeSeries'
135 (Rmetrics Core Team 2015), and 'msm' (Jackson 2015). The decline-curve datasets and R scripts for
136 this study are uploaded in Appendix S1 and S2.

137 We subsequently retrieved information for each population on several anthropogenic
138 pressures, species-specific and time-series related characteristics (see Table 1 for description and
139 sources), which we hypothesised might influence decline-curve dynamics and removed all decline-
140 curves with incomplete information. Home range data and population density were retrieved from the
141 PanTHERIA database of mammalian life-history traits (Jones *et al.* 2009). Generation length was
142 retrieved from Pacifici *et al.* (2013). We obtained information on the number of distinct threats
143 affecting each population from the Living Planet Index database (Collen *et al.* 2009). Maximum
144 finite rate of population growth (r_{\max}) was calculated based on Equation 1 from Slade *et al.* (1998),
145 using data on litter size, maximum longevity and age at sexual maturity from Jones *et al.* (2009). We
146 solved this equation using the 'uniroot.all' function in the 'rootSolve' package (Keith *et al.* 2015), and
147 selected the highest r_{\max} value in cases where there was more than one solution. To obtain values for
148 the two spatial variables ('Human Appropriation of Net Primary Productivity as a percentage of Net
149 Primary Productivity' and the 'Human Influence Index') we created buffer polygons with a radius of
150 1, 10 and 60 km around each population's point location using the 'Analysis Tool' available in
151 ArcMap v. 9.3 (ESRI 2008) and calculated the mean value across the buffers using the 'Zonal
152 Statistics' tool. We chose this particular range of buffer sizes as they correspond to the 25th, 50th and
153 75th percentile (rounded-up to the nearest tenth) of home range sizes in km² across the species with
154 available home range data in the filtered dataset (n=21).

155 A Kruskal Wallis test (Kruskal & Wallis 1952) confirmed there were no statistically
156 significant differences between the mean values at different buffer sizes, therefore we continued the
157 analysis at the 10 km level (see Table S3 in Supplementary Information). Spearman-rank tests
158 (Spearman 1904) were carried out to test for co-linearity between continuous explanatory variables
159 (Table S4 in Supporting Information), and those with a correlation coefficient of greater than 0.7 were
160 removed from the analysis, based on the most commonly used threshold (Dormann *et al.* 2013).

161

162 *Statistical analysis*

163 We first investigated the presence of spatial autocorrelation across each decline-curve by
164 creating a distance-based neighbours list using the 'dnearneigh' function in the package 'spdep'
165 (Bivand 2009). We tested several cut-off distances, from 10 to 100 km, and selected the minimum
166 distance for which all points were connected to at least another one. We then used the 'nb2listw'
167 function from 'spdep' to supplement the neighbours list with two different spatial weights (row-
168 standardised and binary weightings) to characterise the relationships between neighbouring points.
169 Both spatially-weighted neighbour lists were then used in Moran's I and Geary's C tests on the
170 response variable of interests, through the functions 'moran.test' and 'geary.test' from 'spdep'. We ran
171 both Moran's and Geary's tests as the former is more sensitive to extreme values, and the latter is more
172 sensitive to differences in small neighbourhoods.

173 Given that evolutionarily related species and populations are not statistically independent
174 (Felsenstein 1985), we tested whether the distribution of each decline-curve type was phylogenetically
175 correlated using the D statistic (through the 'phylo.d' function in the 'caper' package; Orme *et al.* 2014)
176 based on Fritz *et al.* (2009)'s updated mammalian phylogenetic supertree (Appendix S1). If D was
177 less than 0, this would indicate that species that were more closely related were more likely to decline
178 in the same way, thus necessitating to account for phylogenetic pattern in subsequent statistical
179 analyses.

180 We then modelled the presence/absence of each decline-curve type in relation to the variables
181 listed in Table 1 using generalised linear mixed models with binomial error structures (using the
182 ‘lme4’ package in R; Bates, Maechler & Bolker 2011). We also investigated the impact of
183 misdiagnosing exponential concave declines as quadratic declines by re-running the analysis for all
184 concave declines combined. We did this based on Di Fonzo *et al.* (2013)’s result that exponential
185 concaves declines had a higher chance of misdiagnosis under simulated census error compared to
186 other decline-types. We selected a mixed modelling framework (with “species” and “biogeographic
187 realm” as random effects) to take into account the non-independent, nested structure of the decline-
188 curve data, with multiple populations of the same species from the same region. To address model
189 convergence problems, some of the explanatory variables were scaled where required. We used a
190 multi-model inference approach (Burnham & Anderson 2004) to compare models with all
191 combinations of explanatory variables using the ‘dredge’ function in the ‘MuMIn’ R package (Bartón
192 2014), and calculated model-average coefficients for the parameters included in the top models, i.e.
193 those with a difference of less than 2 AICc. Since the binomial decline-curve type data were not
194 expected to occur under any specific statistical distribution we did not need to test for overdispersion.
195 We identified the variables which had a consistent effect on the presence of each decline-curve type
196 based on whether the 95% confidence interval around their model-averaged coefficients crossed 0 (i.e.
197 we assessed those that did not cross zero as having a consistent effect).

198

199 **RESULTS**

200 Although quadratic convex and combined concave decline-curves exhibited a higher degree
201 of phylogenetic non-randomness compared to the other decline-curve types (Table S5; their D
202 statistics were approximately 0), we did not account for phylogenetic structure in subsequent analyses
203 as this was neither a strong phylogenetic signal, nor supported by a large sample size (n=35 and 58).
204 Spatial autocorrelation was also absent across decline-curves (based on Moran's I and Geary's C tests;
205 all p-values > 0.1; Fig. 2.). We identified 20 plausible models which described quadratic convex

206 decline-curves with less than 2 AICc difference, containing a total of nine parameters in a variety of
207 additive interactions (Tables 2 and S6). We found that only one time-series characteristic consistently
208 explained the presence of quadratic convex decline-curves, with the remaining time-series descriptors,
209 biological traits and anthropogenic measures being less important. Specifically, we found that
210 quadratic convex declines were associated with a change in trajectory towards the start of the time-
211 series (inferred from the negative ‘proximity to end’ estimate; Table 2). The presence of quadratic
212 concave declines was best explained by 23 models containing additive interactions between a total of
213 nine parameters (Tables 3 and S7). “Proximity to end” was the only parameter that was consistently
214 associated with the presence of quadratic concave declines (with a positive model-averaged estimate),
215 suggesting that this cure-type is more likely to occur towards the end of a population time-series. We
216 found that the presence of exponential concave declines was best explained by 58 models, with a
217 combination of 12 variables in additive interactions (Tables 4 and S8). None of these demonstrated a
218 consistent effect on the presence of exponential concave declines. When we combined concave
219 declines together in one category, their presence was best explained by 11 models, with a combination
220 of 7 variables in additive interactions, in addition to the null model (Table S9). None of these had a
221 consistent effect on the presence of this particular decline category.

222

223 **DISCUSSION**

224 Our broad scale study of the distribution of different wildlife population decline-curves in
225 relation to species-specific biological, anthropogenic, and time-series descriptor characteristic
226 predictors demonstrates a novel association with useful management implications. We identify a key
227 time-series characteristic associated with the presence of quadratic convex and quadratic concave
228 declines, which can be explained in the context of different threatening processes. Quadratic convex
229 declines were more likely to occur towards the start of the time-series: a phenomenon that could
230 coincide with the appearance of a novel threat (Mace *et al.* 2010). Quadratic concave declines,
231 instead, were more likely at the end of the analysed time-series. When a new pressure appears, there

232 are four possible responses of a population: it may a) decline and then recover, b) decline to
233 extinction, c) decline and stabilise, or d) be unaffected. Early in this process, quadratic convex
234 declines will be more likely, especially under severe or increasing pressures (e.g. an accelerating rate
235 of habitat conversion). Over the course of time, as the pressure stabilises or reduces, a population that
236 has not declined to extinction must either recover or stabilise, resulting in a concave (or decelerating)
237 curve. The quadratic convex decline-curve type is also the least prevalent across our time-series
238 dataset (compared to concave declines), which may be a result of a ‘filter effect’ (Balmford 1996)
239 causing an inherent bias against the identification of quadratic convex declines. Populations that
240 declined in a quadratic convex manner in the past may have done so too quickly for monitoring to
241 take place (exemplified in the Indian Gyps vultures decline; Prakash *et al.* 2012), or population
242 monitoring may have only started following a severe decline, thereby missing earlier quadratic
243 convex sections.

244 The tendency for quadratic convex declines to occur in the beginning of population time-
245 series means that its identification could act as a signal for a novel threat, following which increased
246 monitoring in combination with rapid conservation effort focussing on threat abatement should be put
247 in place. The fact that quadratic convex declines have been diagnosed with high levels of accuracy
248 under simulated deteriorations in data quality (Di Fonzo, Collen & Mace 2013) is a further reason to
249 support its efficacy as a trigger for interventions. Instead, if concave declines were detected, it could
250 be inferred that the population has already undergone a period of severe decline, from which its rate
251 of decline is slowing or even recovering. The presence of this decline type suggests a different type
252 of management strategy might be required, focussed on supporting recovery (e.g. through improving
253 the species’ habitat). The identification of different decline-curves therefore represents a novel
254 trigger for adaptive management practices (*sensu* Walters 1986), which should be considered in
255 addition to recently proposed measures of “percentage decline in population size, duration of
256 population decline, loss of numbers of subpopulations, or reduction in the distribution of a species”
257 (Lindenmayer, Pigott & Wintle 2013).

258

259 Our analyses do not pick up any relationship between body mass and severe quadratic convex
260 declines, which we had hypothesised as more likely in larger species with an intrinsically higher risk
261 of extinction. Similarly, we found no relation between species with lower r_{\max} (i.e. of slower life-
262 history speed, with greater risk of extinction) and a higher likelihood of quadratic populations
263 declines. Such lack of associations may be due to the low number of quadratic convex declines in this
264 dataset and warrants further investigation. A further characteristic of this dataset which may preclude
265 these associations is that the species included are generally on the slower scale of the mammalian life-
266 history speed continuum, thus reducing the statistical power of our analyses. It would be valuable to
267 follow-up these findings by collecting information on the intraspecific variation in life-history
268 characteristics across the various populations (as identified in Gonz lez-Su rez & Revilla 2013) in
269 order to obtain more precise estimates for such decline-curve associations.

270 Statistical analysis of the distribution of decline-curve types across IUCN Red List extinction-
271 risk categories did not reveal any clear patterns. Contrary to expectation, more severe, quadratic
272 convex declines were no more likely to occur in populations of more threatened species than species
273 with lower extinction risk, despite IUCN Criteria A being based on ‘high population decline rate’.
274 The inconsistency between decline-curve severity and species extinction risk may be explained by the
275 fact that percentage loss in population size and population decline-curve type measure two different
276 processes. The first metric considers the species’ risk of extinction based on the total reduction in
277 population abundance, whereas the latter provides information on how the rate of population decline
278 changes over time. This result highlights how determining populations’ decline-curve type could be a
279 valuable refinement to IUCN Criterion A, indicating a higher risk of extinction for species with
280 population(s) declining at an accelerating rate (Di Fonzo, Collen & Mace 2013).

281 Some potential limitations of the information used here may have affected our findings.
282 Firstly, there was a temporal mismatch between individual population time-series and the predictors
283 of anthropogenic pressure (i.e. HII and HANNP) that will have reduced their explanatory power. The
284 population time-series used in this analysis were recorded between 1950 and 2010, ranging across all
285 decades, whereas the human pressure datasets provided single “snapshots” of the populations’ local

286 conditions that may not represent the pressures affecting the population during the time it was
287 monitored. Secondly, population abundance estimates were compiled from numerous sources, using a
288 variety of monitoring methods and sampling effort, including potential observation errors that may
289 have obscured our ability to correctly categorise decline-curves (as described in Solow 1998; Knappe
290 & de Valpine 2012). Our analyses were also limited to the time-frame over which the data were
291 collected, preventing us from assessing the declines with respect to a historical population baseline
292 (recommended by Porszt *et al.* 2012; d'Eon-Eggertson, Dulvy & Peterman 2014) or over a period of
293 three generation lengths (recommended by the IUCN Standards and Petitions Subcommittee 2010).
294 This may have reduced our ability to diagnose declining populations to begin with, however would
295 not have subsequently affected the analysis. Additionally, our study did not take into account the
296 effect of possible conservation actions on population dynamics, which could have potentially biased
297 our decline-curve results. The paucity of information on the presence and timing of conservation
298 actions across the dataset prevented us from using it within a comparative analysis; however its
299 possible influence on population dynamics merits future investigation through more detailed case-
300 studies. Finally, we included a high number of explanatory variables in our models (with respect to
301 sample size), which may have resulted in potential model overfitting. To reduce the chances of this
302 occurring, we recommend augmenting the dataset through an updated search for suitable population
303 time-series, expanding the study to include data from more animal taxa. A larger dataset would
304 enable division of the time-series into training and testing sets, maximising performance on the
305 training set and testing its efficacy on the unseen portion of data.

306 In addition to acting as a novel type of conservation trigger, dividing observed mammal
307 population decline-curve types into categories of increasing decline severity has the potential to
308 provide important insights for wildlife management. Although not a prioritisation mechanism on its
309 own, differences in decline-type could be incorporated within Criterion A of the IUCN Red List as a
310 more continuous indicator of the urgency with which species' population declines need addressing
311 (while also considering the potential costs and probability of success associated with their recovery).
312 For example, species with a greater number of severe declines could be allocated a higher risk of

313 extinction within the same Red List category, despite not having met the criteria for moving up a
314 category at the species-level. Assessing differences in population decline-curve dynamics could also
315 be useful for prioritising Red List (re)assessments, where an elevated presence of quadratic convex
316 population declines could instigate a closer evaluation of a species' extinction risk. We acknowledge
317 that such changes in the IUCN extinction risk assessment protocol might be difficult to implement
318 unanimously due to differences in the availability of population time-series data for highly threatened
319 species and budget limitations to monitoring additional populations. Extinction-risk categorisations
320 which include information on population decline-curve type may therefore be of greater use to
321 local/regional assessments, where the data is generally of higher resolution.

322 Our study illustrates how the identification of different decline-curve types can provide a
323 signal for a change in management action: quadratic convex declines could be used to trigger rapid
324 conservation action to prevent potential extinctions, while the identification of quadratic concave
325 dynamics could promote increased conservation effort towards the recovery of dwindling populations.
326 In order to confirm the efficacy of these decline-curve types as signals for management change, we
327 recommend performing this analysis over a much wider sample of population time-series, both
328 already collected and in the process of being monitored. Further testing on the power to detect
329 differences in decline dynamics in wild populations will also be required (sensu Nichols & Williams
330 2006).

331

332

333

334 **ACKNOWLEDGEMENTS**

335 This study was initially supported through a U.K. Natural Environment Research Council PhD
336 studentship to M.D.F, followed by funding from the Australian Government's National
337 Environmental Research Program and the Australian Research Council Centre of Excellence for

338 Environmental Decisions. B.C. was partly supported by the Rufford Foundation. We thank the
339 Global Mammal Assessment lab at La Sapienza University, Rome, for useful discussions regarding
340 the preliminary results of this paper, Luca Borger and Ana Nuno for statistical advice, Jonas
341 Geldmann and Monika Böhm for support with spatial data manipulation, and Edd Hammill for
342 comments on an earlier version of this manuscript.

343

344

345

For Peer Review

346 **DATA ACCESSIBILITY**

347 - The mammalian supertree will be available in Appendix S1; originating from Fritz et al. (2009).

348 DOI: 10.1111/j.1461-0248.2009.01307.x

349 - Raw decline-curve datasets will be uploaded in Appendix S1

350 - R scripts for the comparative analyses are uploaded as Appendix S2

351

352

353

354

For Peer Review

355 REFERENCES

- 356 Allee, W.C. (1931) *Animal Aggregations. A Study in General Sociology*. University of Chicago Press,
357 Chicago.
- 358 Balmford, A. (1996) Extinction filters and current resilience: the significance of past selection
359 pressures for conservation biology. *Trends in Ecology and Evolution*, **11**, 193-196.
- 360 Bartón, K. (2014) Package 'MuMIn'. *Comprehensive R Archive Network, Version 1.10.0*.
- 361 Bates, D., Maechler, M. & Bolker, B. (2011) Package 'lme4'. *Comprehensive R Archive Network*,
362 *Version 0.999375-42*.
- 363 Bivand, R. (2009) The spdep package. *Comprehensive R Archive Network, Version 0.4-34*.
- 364 Burnham, K.P. & Anderson, D.R. (2004) Multimodel inference: Understanding AIC and BIC in model
365 selection *Sociological Methods & Research*, **33**, 261-304.
- 366 Ceballos, G. & Ehrlich, P.R. (2002) Mammal population losses and the extinction crisis. *Science*, **296**,
367 904-907.
- 368 Collen, B., Loh, J., Holbrook, S., McRae, L., Amin, R. & Baillie, J.E.M. (2009) Monitoring Change in
369 Vertebrate Abundance: the Living Planet Index. *Conservation Biology*, **23**, 317-327.
- 370 Collen, B., McRae, L., Deinet, S., De Palma, A., Carranza, T., Cooper, N., Loh, J. & Baillie, J.E.M. (2011)
371 Predicting how populations decline to extinction. *Philosophical Transactions of the Royal*
372 *Society of London B*, **366**, 2577-2586.
- 373 Cowlshaw, G., Pettifor, R.A. & Issac, N.J.B. (2009) High variability in patterns of population decline:
374 the importance of local processes in species extinctions. *Proceedings of the Royal Society of*
375 *London B*, **276**, 63-69.
- 376 d'Eon-Eggertson, F., Dulvy, N.K. & Peterman, R.M. (2014) Reliable identification of declining
377 populations in an uncertain world. *Conservation Letters*.
- 378 Di Fonzo, M., Collen, B. & Mace, G., M. (2013) A new method for identifying rapid decline dynamics
379 in wild vertebrate populations. *Ecology and Evolution*, **3**, 2378–2391.
- 380 Dormann, C.F., Elith, J., Bacher, S., Buchmann, C., Carl, G., Carré, G., Marquéz, J.R.G., Gruber, B.,
381 Lafourcade, B., Leitão, P.J., Münkemüller, T., McClean, C., Osborne, P.E., Reineking, B.,
382 Schröder, B., Skidmore, A.K., Zurell, D. & Lautenbach, S. (2013) Collinearity: a review of
383 methods to deal with it and a simulation study evaluating their performance. *Ecography*, **36**,
384 27-46.
- 385 Drake, J.M. & Griffen, B.D. (2010) Early warning signals of extinction in deteriorating environments.
386 *Nature*, **467**, 456-459.
- 387 Felsenstein, J. (1985) Phylogenies and the comparative method. *The American Naturalist*, **125**, 1-15.
- 388 Fritz, S.A., Bininda-Emonds, O.R.P. & Purvis, A. (2009) Geographical variation in predictors of
389 mammalian extinction risk: big is bad, but only in the tropics. *Ecology Letters*, **12**, 538-549.
- 390 Gonzlález-Suárez, M. & Revilla, E. (2013) Variability in life-history and ecological traits is a buffer
391 against extinction in mammals. *Ecology Letters*, **16**, 242-251.
- 392 Imhoff, M.L., Bounoua, L., Ricketts, T., Loucks, C., Harris, R. & Lawrence, W.T. (2004) Global patterns
393 in human consumption of net primary production. *Nature*, **429**, 24.
- 394 Institute of Zoology of the Ministry of Education and Science of the Republic of Kazakhstan (2011)
395 Saiga antelope time-series data.
- 396 IUCN (2001) IUCN Red List categories and criteria: version 3.1. (ed. IUCN). IUCN Species Survival
397 Commission, Gland, Switzerland and Cambridge, United Kingdom.
- 398 IUCN Standards and Petitions Subcommittee (2010) Guidelines for Using the IUCN Red List
399 Categories and Criteria. Version 8.1.
- 400 Jackson, C. (2015) Package 'msm'. *Comprehensive R Archive Network, Version 1.5*.
- 401 Jones, K.E., Bielby, J., Cardillo, M., Fritz, S.A., O'Dell, J., Orme, C.D.L., Safi, K., Sechrest, W., Boakes,
402 E.H., Carbone, C., Connolly, C., Cutt, M.J., Foster, J.K., Grenyer, R., Habib, M., Plaster, C.A.,
403 Price, S.A., Rigby, E.A., Rist, J., Teacher, A., Bininda-Emonds, O.R.P., Gittleman, J.L., Mace, G.,
404 M. & Purvis, A. (2009) PanTHERIA: a species-level database of life history, ecology, and
405 geography of extant and recently extinct mammals. *Ecology*, **90**, 2648.

- 406 Keith, D., Akçakaya, H.R., Butchart, S.H.M., Collen, B., Dulvy, N.K., Holmes, E.E., Hutchings, J.A.,
 407 Keinath, D., Schwartz, M.K., Shelton, A.O. & Waples, R.S. (2015) Temporal correlations in
 408 population trends: Conservation implications from time-series analysis of diverse animal
 409 taxa. *Biological Conservation*, **192**, 247-257.
- 410 Knappe, J. & de Valpine, P. (2012) Are patterns of density dependence in the Global Population
 411 Dynamics Database driven by uncertainty about population abundance? *Ecology Letters*, **15**,
 412 17-23.
- 413 Kruskal, W.H. & Wallis, W.A. (1952) Use of ranks in one-criterion variance analysis. *Journal of the
 414 American Statistical Association*, **260**, 583-621.
- 415 Lindenmayer, D.B., Pigott, M.P. & Wintle, B.A. (2013) Counting the books while the library burns:
 416 why conservation monitoring programs need a plan for action. *Frontiers in Ecology and the
 417 Environment*, **11**, 549–555.
- 418 Mace, G., M., Collen, B., Fuller, R.A. & Boakes, E.H. (2010) Population and geographic range
 419 dynamics: Implications for conservation planning. *Philosophical Transactions of the Royal
 420 Society of London B*, **365**, 3743-3751.
- 421 Mazerolle, M.J. (2015) Package 'AICcmodavg'. *Comprehensive R Archive Network, Version 2.0-3*.
- 422 Nichols, J.D. & Williams, B.K. (2006) Monitoring for conservation *Trends in Ecology and Evolution*, **21**,
 423 668-673.
- 424 Orme, D., Freckleton, R., Thomas, G., Petzoldt, T., Fritz, S., N., I. & Pearse, W. (2014) Package 'caper'.
 425 *Comprehensive R Archive Network, Version 0.5.2*.
- 426 Pacifici, M., Santini, L., Di Marco, M., Baisero, D., Francucci, L., Grotolo Marasini, G., Visconti, P. &
 427 Rondinini, C. (2013) Generation length for mammals. *Nature Conservation*, **5**, 89-94.
- 428 Petris, G. (2015) Package 'dlm'. *Comprehensive R Archive Network, Version 1.1-4*.
- 429 Porszt, E.J., Peterman, R.M., Dulvy, N.K., Cooper, A.B. & Irvine, J.R. (2012) Reliability of indicators of
 430 decline in abundance. *Conservation Biology*, **26**, 894-904.
- 431 Prakash, V., Bishwakarma, M.C., Chaudhary, A., Cuthbert, R., Dave, R., Kulkarni, M., Kumar, S.,
 432 Paudel, K., Ranade, S., Shringarpure, R. & Green, R.E. (2012) The population decline of Gyps
 433 vultures in India and Nepal has slowed since veterinary use of Diclofenac was banned. *PLoS
 434 one*, **7**, e49118.
- 435 Purvis, A., Agapow, P.-M., Gittleman, J.L. & Mace, G., M. (2000) Nonrandom extinction and the loss
 436 of evolutionary history. *Science*, **288**, 328-330.
- 437 R Development Core Team (2015) R: A language and environment for statistical computing. R
 438 foundation for Statistical Computing, Vienna.
- 439 Rmetrics Core Team (2015) The timeSeries package. *Comprehensive R Archive Network, Version
 440 3012.99*.
- 441 Sanderson, E.W., Jaiteh, M., Levy, M.A., Redford, K.H., Wannebo, A.V. & Woolmer, G. (2002) The
 442 Human Footprint and the Last of the Wild. *BioScience*, **52**, 891-904.
- 443 Scheffer, M., Bascompte, J., Brock, W.A., Brovkin, V., Carpenter, S.R., Dakos, V., Held, H., van Nes,
 444 E.H., Rietkerk, M. & Sugihara, G. (2009) Early-warning signals for critical transitions. *Nature*,
 445 **461**, 53-59.
- 446 Schipper, J., Chanson, J.S., Chiozza, F., Cox, N.A., Hoffmann, M., Katariya, V., Lamoreux, J., Rodrigues,
 447 A.S.L., Stuart, S.N., Temple, H.J., Baillie, J., Boitani, L., Lacher, T.E., Mittermeier, R.A., Smith,
 448 A.T., Absolon, D., Aguiar, J.M., Amori, G., Bakkour, N., Baldi, R., Berridge, R.J., Bielby, J.,
 449 Black, P.A., Blanc, J.J., Brooks, T.M., Burton, J.A., Butynski, T.M., Catullo, G., Chapman, R.,
 450 Cokeliss, Z., Collen, B., Conroy, J., Cooke, J.G., da Fonseca, G.A.B., Derocher, A.E., Dublin,
 451 H.T., Duckworth, J.W., Emmons, L., Emslie, R.H., Festa-Bianchet, M., Foster, M., Foster, S.,
 452 Garshelis, D.L., Gates, C., Gimenez-Dixon, M., Gonzalez, S., Gonzalez-Maya, J.F., Good, T.C.,
 453 Hammerson, G., Hammond, P.S., Happold, D., Happold, M., Hare, J., Harris, R.B., Hawkins,
 454 C.E., Haywood, M., Heaney, L.R., Hedges, S., Helgen, K.M., Hilton-Taylor, C., Hussain, S.A.,
 455 Ishii, N., Jefferson, T.A., Jenkins, R.K.B., Johnston, C.H., Keith, M., Kingdon, J., Knox, D.H.,
 456 Kovacs, K.M., Langhammer, P., Leus, K., Lewison, R., Lichtenstein, G., Lowry, L.F., Macavoy,

- 457 Z., Mace, G.M., Mallon, D.P., Masi, M., McKnight, M.W., Medellín, R.A., Medici, P., Mills, G.,
458 Moehlman, P.D., Molur, S., Mora, A., Nowell, K., Oates, J.F., Olech, W., Oliver, W.R.L., Oprea,
459 M., Patterson, B.D., Perrin, W.F., Polidoro, B.A., Pollock, C., Powel, A., Protas, Y., Racey, P.,
460 Ragle, J., Ramani, P., Rathbun, G., Reeves, R.R., Reilly, S.B., Reynolds, J.E., Rondinini, C.,
461 Rosell-Ambal, R.G., Rulli, M., Rylands, A.B., Savini, S., Schank, C.J., Sechrest, W., Self-Sullivan,
462 C., Shoemaker, A., Sillero-Zubiri, C., De Silva, N., Smith, D.E., Srinivasulu, C., Stephenson, P.J.,
463 van Strien, N., Talukdar, B.K., Taylor, B.L., Timmins, R., Tirira, D.G., Tognelli, M.F., Tsytsulina,
464 K., Veiga, L.M., Vié, J.-C., Williamson, E.A., Wyatt, S.A., Xie, Y. & Young, B.E. (2008) The status
465 of the world's land and marine mammals: Diversity, threat, and knowledge. *Science*, **322**,
466 225-230.
- 467 Shoemaker, K.T. & Akçakaya, H.R. (2015) Inferring the nature of anthropogenic threats from long-
468 term abundance records. *Conservation Biology*, **29**, 238–249.
- 469 Slade, N.A., Gomulkiewicz, R. & Alexander, H.M. (1998) Alternatives to Robinson and Redford's
470 method of assessing overharvest from incomplete demographic data. *Conservation Biology*,
471 **12**, 148-155.
- 472 Solow, A.R. (1998) On fitting a population model in the presence of observation error. *Ecology*, **79**,
473 1463-1466.
- 474 Spearman, C. (1904) The proof and measurement of association between two things. *American*
475 *Journal of Psychology*, **15**, 72-101.
- 476 Stearns, S.C. (1983) The influence of size and phylogeny on patterns of covariation among life-history
477 traits in the mammals. *Oikos*, **41**, 173-187.
- 478 Sugiura, N. (1978) Further analysis of the data by Akaike's Information Criterion and the finite
479 corrections. *Communications in Statistics, Theory and Methods*, **A7**, 13-26.
- 480 Walters, C.J. (1986) *Adaptive Management of Renewable Resources*. Macmillan, New York, USA.
- 481 Wildlife Conservation Society & Center for International Earth Science Information Network (2005)
482 Last of the Wild Data Version 2.
- 483 Willis, K.J., Araújo, M.B., Bennett, K.D., Figueroa-Rangel, B., Froyd, C.A. & Myers, N. (2007) How can a
484 knowledge of the past help to conserve the future? Biodiversity conservation and the
485 relevance of long-term ecological studies. *Philosophical Transactions of the Royal Society of*
486 *London B*, **362**, 175-186.
- 487 Wood, S.N. (2006) *Generalized Additive Models: An introduction with R* Chapman & Hall/CRC,
488 Florida.
- 489 Yoccoz, N.G., Nichols, J.D. & Boulinier, T. (2001) Monitoring of biological diversity in space and time.
490 *Trends in Ecology and Evolution*, **16**, 446-453.
- 491
- 492

493 TABLES

494 **Table 1.** Hypothesised predictors of decline-curve type. Bolded variables were included in statistical
 495 modelling following correlation testing.

Variable category	Predictor variable	Description of index (where applicable)	Data source (where applicable)	Hypothesis
Anthropogenic	Human appropriation of Net Primary Productivity (NPP) as a percentage of NPP (HAPNPP; %)	Composite index based on a per capita consumption rate of food and fibre products calculated at country-level (using information from the Food and Agricultural Organisation of the United Nations from 1995). Grid layer at ¼ degree resolution.	Imhoff <i>et al.</i> (2004)	There will be a higher likelihood of severe quadratic convex declines in locations with higher HAPNPP.
	Human Influence Index (HII)	Human pressure metric incorporating indices for population density, land transformation, access and electrical power infrastructure. Full details in Sanderson <i>et al.</i> (2002). Grid layer, at 30 arc second resolution.	Last of the Wild Data Version 2 (Wildlife Conservation Society & Center for International Earth Science Information Network 2005)	There will be a higher likelihood of severe quadratic convex declines in locations with higher HII.

	Threat number	Number of reported threats associated with the time-series (ranged from 1 to 3).		There will be a higher likelihood of severe quadratic convex declines in locations with more threats.
Species-specific biological	IUCN Red List Category	Category indicating species extinction risk: Extinct, Critically Endangered, Endangered, Vulnerable, Near Threatened, or Least Concern.	IUCN (2001)	There will be a higher likelihood of severe quadratic convex declines in populations with higher extinction risk.
	Log adult body mass	Grams	panTHERIA database (Jones <i>et al.</i> 2009).	Heavier species represent longer lived species (Stearns 1983), which have been found at greater risk from extinction compared to faster lived animals (Purvis <i>et al.</i> 2000). Based on this association we would expect a relatively higher frequency of quadratic convex declines within their population time-series.
	Animal population density	Individuals/km ²	panTHERIA database (Jones <i>et al.</i> 2009).	We expect a higher likelihood of severe quadratic convex declines in populations that live at higher density, as these will be more prone to rapid collapse under an Allee effect (Allee 1931).
	Generation length	The weighted mean age of mothers within a population (IUCN Standards and Petitions	Pacifici <i>et al.</i> (2013)	We expect longer-lived species to exhibit a higher frequency of convex declines due to being intrinsically at higher risk of extinction.

		Subcommittee 2010), measured in days.	
	Maximum finite rate of population growth (r_{\max})	Calculated using Eq. 1 in Slade <i>et al.</i> (1998), with data on maximum longevity, number of offspring per year, and age at sexual maturity from Jones <i>et al.</i> (2009). We assumed a 50% female: male ratio in our calculations.	As above, we expect longer-lived species with lower r_{\max} values to exhibit a higher frequency of convex declines due to being intrinsically at higher risk of extinction.
Time-series descriptor	Series fullness	Ratio of number of raw data points with respect to the overall time-series length.	Exponential concave declines require relatively more data for accurate diagnosis (Di Fonzo, Collen & Mace 2013) therefore these may be more likely to be detected in fuller time-series.
	Time-series length	Number of years monitoring took place (calculated from the first to final year of the monitoring period).	Based on the above information, exponential concave declines may also be more likely in longer time-series.
	Slope	Based on a linear regression over each switch-point delimited sections with respect to time.	Quadratic convex declines may be more likely within time-series with more negative slopes, where the external pressures are higher.
	Switch point number	Number of significant switches in dynamics	Quadratic convex and concave declines may be more likely in highly

	over the entire time-series. Switch points were diagnosed following Di Fonzo et al. 2013.	fluctuating time-series than exponential concave declines (are characterised by a longer “tail”).
Mean lambda	Mean change in population abundance over the entire time-series.	Quadratic convex declines may exhibit the most negative change in population abundance over time.
Cumulative lambda	Cumulative change in population abundance over the time-series (calculated by adding up the individual, yearly lambdas).	Quadratic convex declines may exhibit the most negative cumulative change in population abundance over time.
Proximity to end	The final year of the declining section divided by the total length of the time-series (e.g. if the decline occurred from year 8 to year 17 and the entire time-series was 20 years long, “proximity to end” would be 17/20).	Quadratic convex and quadratic concave declines may be more likely to occur towards the start of a time-series (representing increased fluctuations in response to a novel threat) whereas exponential concave declines may be more likely towards the end of a time-series on account of its longer “tail”.

496

497

498 **Table 2.** Results from generalized linear mixed models fitted to quadratic convex declines (n=35).
 499 The table presents the model-average coefficients of the parameters from the most plausible models
 500 (<2 Δ AICc). Bolded parameters indicate those with a statistically significant effect. Parameter
 501 numbers correspond to parameters listed in Table S6.

Number	Parameter	Model averaged estimate	Model averaged lower 95% CI	Model averaged upper 95% CI
	Intercept	-3.806	-10.797	3.186
1	Mean lambda	6.541	-0.423	13.505
2	Proximity to end	-2.856	-5.096	-0.615
3	r_{\max}	-0.509	-1.236	0.219
4	Animal population density	0.464	-0.245	1.173
5	Series fullness	1.233	-0.693	3.158
6	Human Influence Index	-0.393	-1.104	0.318
7	Slope	0.268	-0.383	0.919
8	Threat number	-0.385	-1.119	0.348
9	Human Appropriation of NPP	-0.295	-1.396	0.806

502

503

504

505 **Table 3.** Results from generalized linear mixed models fitted to quadratic concave declines (n=29).
 506 The table presents the model-average coefficients of the parameters from the most plausible models
 507 (<2 Δ AICc). Bolded parameters indicate those with a statistically significant effect. Parameter
 508 numbers correspond to parameters listed in Table S7.

Number	Parameter	Model averaged estimate	Model averaged lower 95% CI	Model averaged upper 95% CI
	Intercept	-2.473	-5.147	0.201
1	Proximity to end	2.601	0.067	5.135
2	r_{\max}	0.414	-0.133	0.961
3	Series fullness	-1.764	-3.855	0.327
4	Threat number	0.468	-0.245	1.181
5	Human Appropriation of NPP	-1.402	-6.818	4.015
6	Switch point number	0.281	-0.271	0.834
7	Slope	0.473	-1.265	2.212
8	Animal population density	-0.309	-1.173	0.555
9	Time-series length	-0.425	-1.187	0.337

509

510

511

512 **Table 4.** Results from generalized linear mixed models fitted to exponential concave declines (n=21).
 513 The table presents the model-average coefficients of the parameters from the most plausible models
 514 (<2 Δ AICc). Bolded parameters indicate those with a statistically significant effect. Parameter
 515 numbers correspond to parameters listed in Table S8.

Number	Parameter	Model averaged estimate (SE)	Model averaged lower 95% CI	Model averaged upper 95% CI
	Intercept	2.858	-3.348	9.063
1	Slope	-0.516	-1.514	0.483
2	Switch point number	-0.512	-1.169	0.145
3	Mean lambda	-5.708	-11.975	0.560
4	Human Appropriation of NPP	0.438	-0.347	1.222
5	Threat number	-0.684	-1.778	0.410
6	Series fullness	1.246	-0.942	3.435
7	Animal population density	-0.394	-1.296	0.508
8	r_{\max}	0.315	-0.257	0.887
9	Cumulative lambda	-0.096	-0.397	0.205
10	Proximity to end	1.247	-1.457	3.951
11	Human Influence Index	-0.315	-1.011	0.381
12	Time-series length	0.913	-3.933	5.760

516

517

518 **Table 5.** Results from generalized linear mixed models fitted to combined concave declines (n=58).
 519 The table presents the model-average coefficients of the parameters from the most plausible models
 520 (<2 Δ AICc). Bolded parameters indicate those with a statistically significant effect. Parameter
 521 numbers correspond to parameters listed in Table S9.

Number	Parameter	Model averaged estimate (SE)	Model averaged lower 95% CI	Model averaged upper 95% CI
	Intercept	2.130	-3.014	7.273
1	Animal population density	-0.528	-1.175	0.119
2	Mean lambda	-4.292	-10.734	2.150
3	r_{\max}	0.471	-0.573	1.515
4	Cumulative lambda	-0.015	-0.052	0.021
5	Switch point number	-0.144	-0.517	0.230
6	Time-series length	-0.166	-0.634	0.302
7	Human Appropriation of NPP	0.285	-0.911	1.481
8	Proximity to end	0.568	-1.428	2.564

522

523

524

525

526

527

528

529

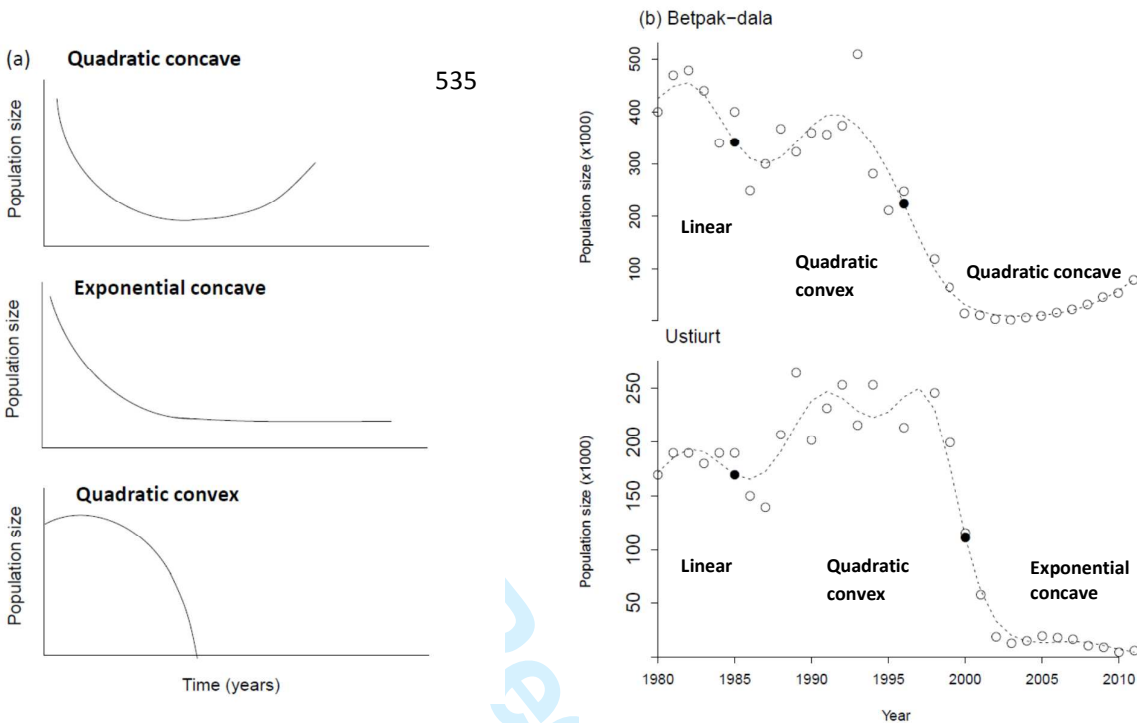
530

531

532

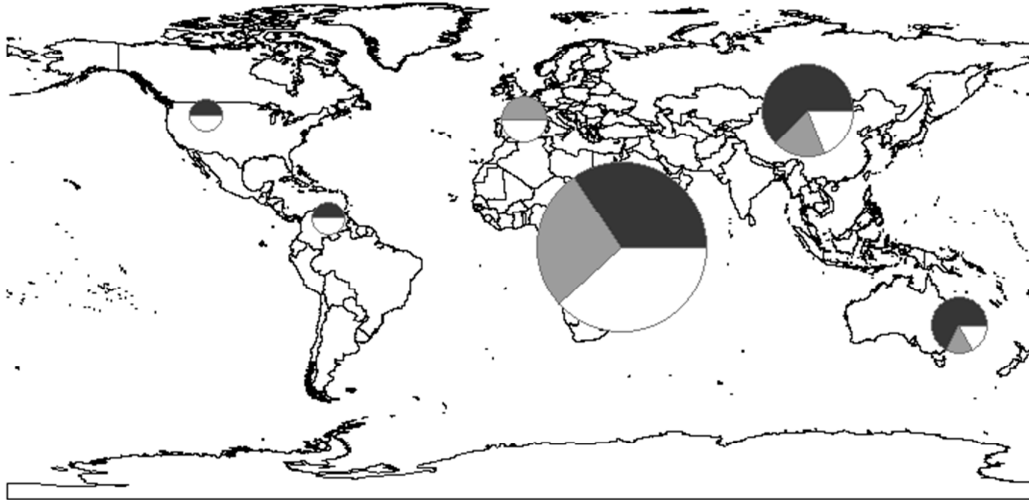
533 **FIGURE**

534



536 **Figure 1.** (a) From top to bottom: Quadratic concave, exponential concave, and quadratic convex
 537 decline patterns found in wildlife populations, associated with simulated decreasing proportional
 538 pressure, constant proportional pressure, and increasing fixed pressure (from Di Fonzo, Collen &
 539 Mace 2013); (b) Exemplary time-series of Saiga populations from Betpak-dala and Ustiurt regions in
 540 Kazakhstan (Institute of Zoology of the Ministry of Education and Science of the Republic of
 541 Kazakhstan 2011). Raw data are indicated by open points, switch points are indicated as closed
 542 points, and dotted lines reflect the smoothed time-series generated from the GAM. The Betpak-dala
 543 population dynamics are best-fit by: (A) linear, (B) quadratic convex, and (C) quadratic concave
 544 curves (from 1980 onwards, separated by switch points), whereas the Ustiurt population dynamics are
 545 best fit by (A) linear, (B) quadratic convex, and (C) exponential concave curves. The statistical output
 546 for the best-fit curves is presented in the Table S1 in Supporting Information.

547



548

549 **Figure. 2.** Terrestrial mammalian decline-curve types grouped according to continent. Dark grey
 550 portions of pie-charts represent quadratic convex declines (most severe), grey portions represent
 551 exponential concave declines (mid-severity) and white represent quadratic concave declines (least
 552 severe). The size of the pie-chart is relative to the number of declines per continent (n= 55 in Africa,
 553 n=16 in Asia, n= 2 in North America, n= 4 in Europe, n=2 for Latin America and the Caribbean and 6
 554 in Australasia).

555